Proc. Natl. Sci. Counc. ROC(A)
Vol. 21, No. 5, 1997. pp. 493-504

Measurements of Temporal and Spatial Characteristics of In-Cylinder Turbulent Flowfields

CHE-WUN HONG AND DER-GEE CHEN

Department of Power Mechanical Engineering
National Tsing Hua University
Hsinchu, Taiwan, R.O.C.

(Received January 6, 1997; Accepted April 8, 1997)

ABSTRACT

This paper describes hardware and software technology developed at Tsing Hua University to measure the in-cylinder temporal and spatial characteristics of the turbulent flowfield inside a transparent engine, using a two-probe fiber laser Doppler velocimeter (FLDV). A single-cylinder four-stroke research engine, whose liner is transparent, was operated under 500 rpm motoring conditions. A traverse table was designed which combines two fiber optical probes and is capable of both 3-D single-point and 1-D two-point measurements of the velocity field. The former measurement was taken to determine the mean flow and turbulence intensity (temporal characteristics) while the latter was employed to determine the integral length scales (spatial characteristics) of the turbulent flowfield directly. Statistical algorithms were derived to process the random data. The physical meaning of the experimental results is explained.

Key Words: fiber laser Doppler velocimeter, turbulence intensity, integral length scales

I. Introduction

The in-cylinder air motion of a reciprocating engine is inherently a 3-D, periodic (with cyclic variation), nonstationary turbulent flowfield due to the strong jet flow across the valves and also due to the repeated compression/expansion effects from the moving piston. It has been well proven that the in-cylinder turbulent flow has the potential to further refine the combustion process if certain flow control methods are employed. The major research on this topic has been solidly founded on study of the turbulent flow characteristics, both temporal and spatial (Reynolds, 1980; Heywood, 1987). The mean flow, turbulence intensity and integral length scale are of fundamental importance in understanding the complexity of the flow physics. They have been also used as major parameters to compare simulation and experimental results in turbulence studies (Abraham *et al.*, 1985; Coz *et al.*, 1990; Han *et al.*, 1996). The integral length scale is a quantitative measure of a distance characteristic of turbulent transport while turbulence intensity is a measure of the characteristic speed of transport over the characteristic distance.

For the past twenty years, a substantial amount of effort has been focused on measurement of the turbulence characteristics inside an engine cylinder using either the hot wire anemometry (HWA) or the non-intrusive laser diagnostic methods (Witze, 1980; Dyer, 1985; Sweetland and Reitz, 1994). The majority of the in-cylinder velocity measurements reported in the literature mainly focus on the temporal characteristics, such as the mean flow and turbulence intensity (Cantania *et al.*, 1992; Liou and Santavicca, 1983, 1985; Liou *et al.*, 1984; Hong and Huang, 1995; Hong and Tzeng, 1996). The initial turbulence length scale estimates were made by relating the length scale to the time scale using a rude hypothesis (called an "indirect length scale" in this paper). Several attempts at direct measurement of the in-cylinder integral length scales have been carried out. The methods have included flying HWA (Dinsdale *et al.*, 1988), scanning LDV (Glover *et al.*, 1988a, 1988b), the laser homodyne principle (Ikegami *et al.*, 1985, 1987), and the latest single-probe two-point method (Fraser and Bracco, 1988, 1989). The most simple and effective way is the single-probe two-point method which elongates the focused probe volume. Scattered light is collected from two distinct locations within the elongated probe volume. This device is easy to construct, but the range of the measured length scale is limited by the axial length of the elongated volume, say 5 mm according to the literature.

This paper introduces a new configuration of

a two-probe FLDV system to measure the mean flow, turbulence intensity and length scale at the same time. The objective of this research was to study the temporal and spatial characteristics of the in-cylinder turbulent flowfield of a motoring four-stroke spark-ignition engine. In addition, the results of this work also provide a database for verification of in-cylinder computational fluid dynamics (Kong and Hong, 1997). An example transparent engine test rig was set up at Tsing Hua University to carry out the research. This paper gives details of the experimental work and analysis of the experimental results.

II. Experimental Apparatus

A Megatech single-cylinder research engine with a 41 mm bore, 51 mm stroke and 4:1 compression ratio was used. It was modified so as to be optically accessible by replacing the liner with a transparent quartz tube. The piston head was trimmed flat in order to simplify the shape of the combustion chamber by making it pan-cake type. The piston rings were made of teflon to reduce the problem of window scuffing. The engine was operated under motoring conditions at 500 rpm without cylinder lubrication. The power source was a DC motor which was capable of both motoring and absorption functions. The detailed specifications of the research engine are shown in Table 1. A schematic diagram of the test rig configuration is shown in Fig. 1. An optical encoder was connected to the front of the crank shaft to generate 720 pulses per revolution. These pulses were processed by a rotating machinery resolver to synchronize the burst detector. The Doppler signal was processed by an autocorrelator, TSI IFA750. An IBM PC 486 was connected to process the large amount of data. A piezo-electric pressure transducer was installed on the cylinder head of the research engine to monitor the in-cylinder performance and also to check the cyclic variation.

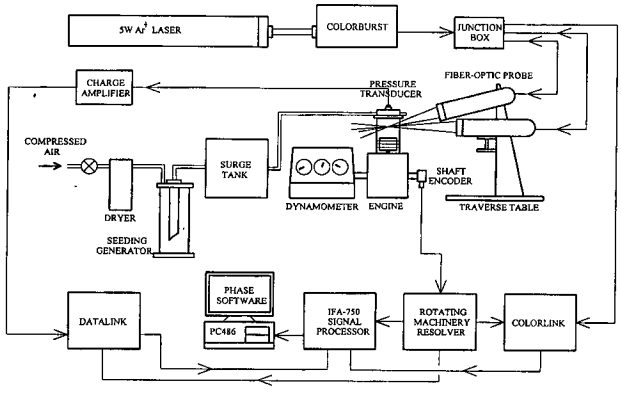

Fig. 1. The schematic configuration of the experimental apparatus.

Table 1. Specifications of the Research Engine

Model	Megatech Mark III
No. of cylinders	1
No. of strokes	4
Bore	41 mm
Stroke	51 mm
Connecting rod length	165 mm
Displacement	68 c.c.
Compression ratio	4
Inlet valve open (IVO)	0° ATDC
Inlet valve closure (IVC)	28° ABDC
Exhaust valve open (EVO)	46° BBDC
Exhaust valve closure (EVC)	13° ATDC

Table 2. Specifications of the Laser Doppler Velocimeter System

LDV manufacturer	TSI
Transmitting lens focal length	green, blue: 499.5 mm purple: 349.8 mm
Beam spacing	50 mm
Beam diameter	2.1 mm
Probe volume dimension (diameter × length)	green, blue: 165.5 μm × 3.4 mm purple: 117.2 μm × 1.7 mm
Effective frequency shift	+ 10 MHz
Signal processor	digital burst correlator TSI IFA 750
Seeding particles	0.7 μm MgO
Laser power source	5 W Ar^+ laser

The major instrument was the FLDV system. Its major specifications are tabulated in Table 2. Basically, this is a two-probe (one four-beam, the other one two-beam) 3-component velocimeter. The system is powered by a 5 Watt argon-ion laser. During testing, the power source was adjusted from 0.5 W to 5 W, depending on the signal-to-noise ratio (SNR). The optical system was able to work as both a 3-D single-point and a 1-D two-point velocity measurement instrument through a traverse stage designed as shown in Fig. 2. For two-point simultaneous measurements, the traverse table was designed to fix the reference probe at the vertical side while the moveable probe could be adjusted along the horizontal axes using another miniature 2-D traverse stage. These two probes had their own focal lengths for both velocity and length scale measurements. For the 3-D single-point measurement, the two probes were perpendicular to each other in a horizontal plane. Figure 3 shows the measurement locations of the flowfield. There were nine points, which were distributed on a plane 10 mm

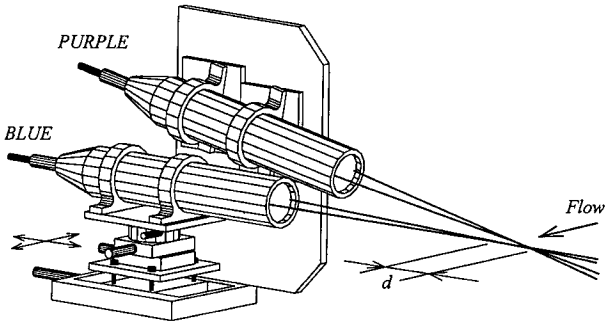

(a) 1-D 2-point measurement

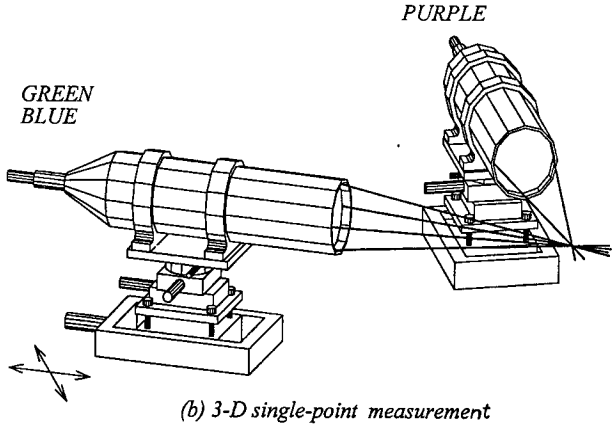

(b) 3-D single-point measurement

Fig. 2. Traverse table design and the relative positions of the fiber optical probes for (a) 1-D 2-point measurement and (b) 3-D single-point measurement.

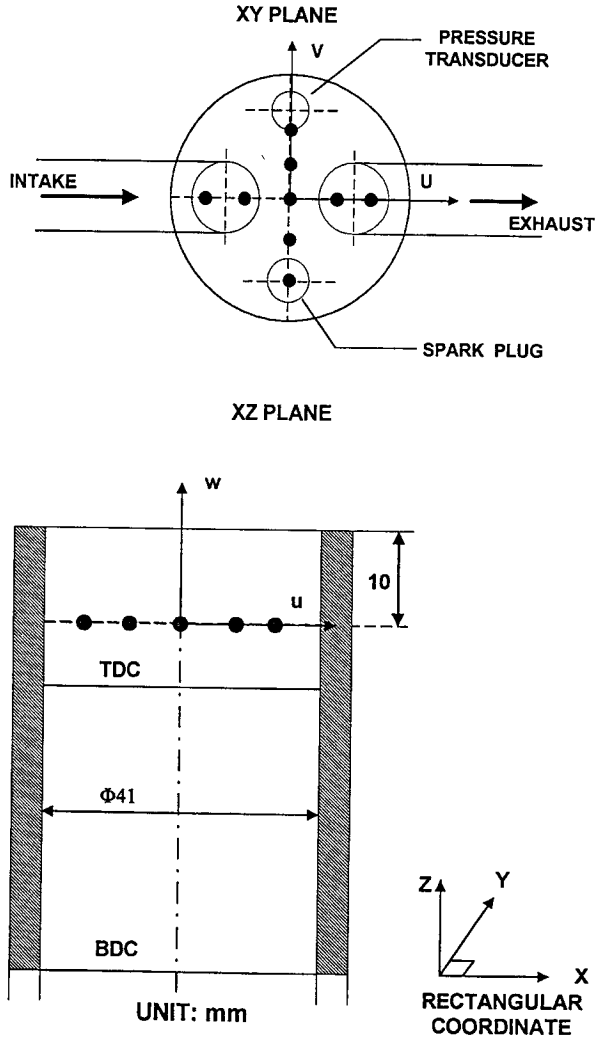

Fig. 3. Measurement locations in the pan-cake type combustion chamber.

below the flat cylinder head. For the length scale measurement, the changeable point moved along the X and Y axes.

III. Analysis of Experimental Data

1. Ensemble Averaged Analysis

Due to the fact that LDV signals occur randomly, a crank angle window is thus defined to be $\overline{\theta} = \theta \pm \Delta\theta/2$. This means that measurements taken within the range $\theta \pm \Delta\theta/2$ are all assigned to the quantity at θ, which is replaced by the crank angle window $\overline{\theta}$. Ensemble averaged analysis uses a traditional statistical algorithm to deal with the periodic phenomenon by lumping all the variations in the cycle together as a fluctuation element. In this technique, the in-cylinder instantaneous velocity, at a specific crank angle $\overline{\theta}$ in a specific cycle i, can be split into an ensemble averaged mean velocity $U_{EA}(\overline{\theta})$ and a fluctuation velocity $u_F(\overline{\theta}, i)$:

$$U(\overline{\theta}, i) = U_{EA}(\overline{\theta}) + u_F(\overline{\theta}, i), \tag{1}$$

where the mean velocity is calculated from many consecutive cycles by

$$U_{EA}(\overline{\theta}) = \frac{1}{N_t(\overline{\theta})} \sum_{i=1}^{N_c} U(\theta \pm \Delta\theta/2, i). \tag{2}$$

The notation N_c is the number of cycles for which data are acquired, and $N_t(\overline{\theta})$ is the total number of measurements within the crank angle window over N_c cycles. The ensemble averaged fluctuation intensity can be, thus, defined as the root mean square (RMS) of the fluctuation velocity:

$$u'_{F,EA}(\overline{\theta}) = \left\{ \frac{1}{N_t(\overline{\theta})} \sum_{i=1}^{N_c} [U(\theta \pm \Delta\theta/2, i) - U_{EA}(\overline{\theta})]^2 \right\}^{1/2} \tag{3}$$

The ensemble averaged analysis is a typical statistical algorithm for periodical flows. Unfortunately, it lumps the turbulence and the fluctuation of cycle-to-cycle variations together. The following technique is used to decompose these two different components.

2. Cycle-Resolved Analysis

In cycle-resolved analysis, the instantaneous velocity is split into a bulk velocity $\overline{U}(\overline{\theta}, i)$ and a turbulence velocity $u_T(\overline{\theta}, i)$:

$$U(\overline{\theta}, i)=\overline{U}(\overline{\theta}, i)+u_T(\overline{\theta}, i). \tag{4}$$

Note that the in-cycle bulk velocity is a function of both the crank angle and the cycle number. When the number of cycles acquired is sufficient for statistical analysis, the mean bulk velocity can be averaged again using the same ensemble average algorithm as mentioned in the previous section; i.e.,

$$\overline{U}_{EA}(\overline{\theta})=\frac{1}{N_R}\sum_{i=1}^{N_R}\overline{U}(\overline{\theta}, i), \tag{5}$$

where N_R refers to the cycle number suitable for cycle-resolved analysis.

Using this technique, the difference between the in-cycle bulk velocity and the ensemble mean bulk velocity can be explained as the bulk velocity fluctuation (or cyclic variation):

$$\hat{U}(\overline{\theta}, i)=\overline{U}(\overline{\theta}, i)-\overline{U}_{EA}(\overline{\theta}). \tag{6}$$

Compared with the ensemble averaged analysis, the fluctuation velocity $u_F(\overline{\theta}, i)$ is, in fact, the sum of the cycle variation and the turbulence velocity. In mathematical form, it is expressed as

$$u_F(\overline{\theta}, i)=\hat{U}(\overline{\theta}, i)+u_T(\overline{\theta}, i). \tag{7}$$

The RMS of the bulk velocity fluctuation is defined as

$$\overline{U}_{RMS}(\overline{\theta})=\left\{\frac{1}{N_R}\sum_{i=1}^{N_R}[\overline{U}(\overline{\theta}, i)-\overline{U}_{EA}(\overline{\theta})]^2\right\}^{1/2}. \tag{8}$$

This indicates the fluctuation intensity of the cycle variations of the in-cylinder flowfield. The turbulence intensity is defined as the RMS of the turbulence velocity. It can be expressed as follows:

$$u'_{T,EA}(\overline{\theta})=\left\{\frac{1}{N_t(\overline{\theta})}\sum_{i=1}^{N_R}[U(\theta\pm\Delta\theta/2, i)-\overline{U}(\overline{\theta}, i)]^2\right\}^{1/2} \tag{9}$$

In this study, a low-pass frequency filtering method (Liou and Santavicca, 1985) was adopted to decompose the low frequency cycle variation from the bulk velocity. The Fast Fourier transform (FFT) and inverse FFT techniques were employed to process the random data in the frequency domain. A cut-off frequency at 500 Hz was chosen to set the criterion for the high frequency turbulence and the low frequency cyclic variation.

3. Temporal Autocorrelation Coefficient

To describe the in-cylinder nonstationary turbulent flowfield, integral time scales and length scales are typical quantities used to characterize the random phenomenon. Time scales indicate the transit time of the eddies while length scales indicate the size of the eddies. Both scales can be evaluated through the definition of the temporal autocorrelation coefficient. That is,

$$R_T(\overline{\theta}, \phi)=\frac{1}{N_c}\frac{\sum_{i=1}^{N_c}u(\overline{\theta}, i)\cdot u(\overline{\theta}+\phi, i)}{u'_{EA}(\overline{\theta})\cdot u'_{EA}(\overline{\theta}+\phi)}, \tag{10}$$

where ϕ refers to phase angle with respect to $\overline{\theta}$. From the definition, the temporal autocorrelation coefficient is a function of the crank angle and the phase angle. For ensemble averaged analysis, u means the fluctuation velocity u_F; u'_{EA} means the ensemble averaged fluctuation intensity $u'_{F,EA}$. On the other hand, for cycle resolved analysis, u means the turbulence velocity u_T; u'_{EA} means the ensemble averaged turbulence intensity $u'_{T,EA}$.

Mathematically, the integral time scale is defined as the area below the curve of the temporal autocorrelation coefficient, R_T, with respect to time; i.e.,

$$\tau_I\equiv\int_0^{\infty}R_T(\tau)\,d\tau. \tag{11}$$

The in-cylinder nonstationary turbulent flow is modified to be

$$\tau_I=\int_0^{\phi_{\max}}|R_T(\overline{\theta}, \phi)|\,d\phi, \tag{12}$$

where ϕ_{max} is the maximum phase angle, where the velocity fluctuations are no longer correlated. The integral time scale is an indication of temporal correlation of the velocity fluctuation. For the flow without mean motion, it means the lifetime of large eddies; while for the flow with mean motion, it means the transit time of large eddies passing through a point in the flowfield.

For rough estimation, the length scale can be related to the product of the ensemble averaged velocity and the time scale by Taylor's hypothesis (Hinze, 1975); i.e.,

$$L_I(\overline{\theta}) = |U_{EA}(\overline{\theta})| \cdot \tau_I(\overline{\theta}). \tag{13}$$

This is named as the "indirect length scale" in this paper. This means that it is measured from the single-point method indirectly. The integral length scale indicates the size of the larger eddies in the flowfield; it is also regarded as a characteristic mixing length in some turbulence models (Tennekes and Lumley, 1972).

4. Spatial Autocorrelation Coefficient

In a homogeneous isotropic flowfield, the spatial autocorrelation coefficient can be classified into a lateral correlation coefficient R_g and a longitudinal correlation coefficient R_f. The spatial relation of the corresponding velocity fluctuations of these two coefficients is illustrated in Fig. 4. The lateral correlation coefficient, R_g, and longitudinal correlation coefficient, R_f, in a nonstationary flowfield can be defined as follows:

$$R_g(\overline{\theta}, r_2) = \frac{1}{N_t - 1} \sum_{i=1}^{N_t} \frac{u_1(\overline{\theta}, x_2, i) \cdot u_1(\overline{\theta}, x_2 + r_2, i)}{u'_1(\overline{\theta}, x_2) \cdot u'_1(\overline{\theta}, x_2 + r_2)} \tag{14}$$

and

$$R_f(\overline{\theta}, r_1) = \frac{1}{N_t - 1} \sum_{i=1}^{N_t} \frac{u_1(\overline{\theta}, x_1, i) \cdot u_1(\overline{\theta}, x_1 + r_1, i)}{u'_1(\overline{\theta}, x_1) \cdot u'_1(\overline{\theta}, x_1 + r_1)}, \tag{15}$$

where

x_1, x_2: the fixed points on the axes of X_1, X_2;
r_1, r_2: the distance between the changeable point and the fixed point on the axes of X_1, X_2;
i: the i'th measurement;
N_t: the total number of measurements within the crank angle window $\overline{\theta}$;
u_1: the velocity fluctuation in the direction of the X_1 axis;
u'_1: the velocity fluctuation intensity in the direction of the X_1 axis.

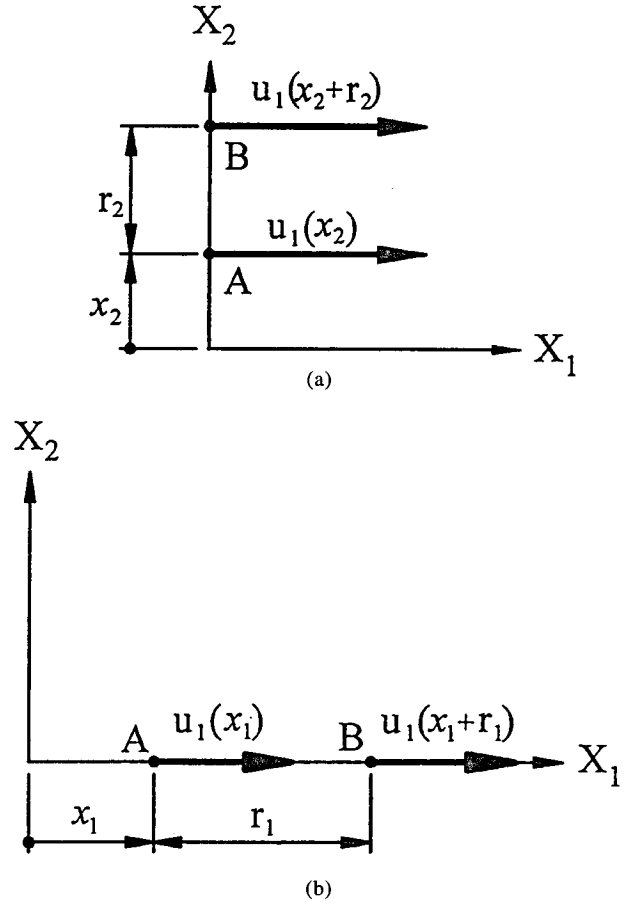

Fig. 4. Spatial relation of the corresponding velocity fluctuations of (a) the lateral correlation coefficient and (b) the longitudinal correlation coefficient.

Since these spatial coefficients can be measured directly using the two-point method described in Section II, the direct integral length scale can be defined as the area below the curve of the spatial autocorrelation coefficient with respect to the seperation distance. In the nonstationary in-cylinder flowfield, the lateral integral length scale can be evaluated by

$$L_g(\overline{\theta}, x_2) = \int_0^{r_2^*} R_g(\overline{\theta}, r_2)\, dr_2, \tag{16}$$

and the longitudinal integral length scale is

$$L_f(\overline{\theta}, x_1) = \int_0^{r_1^*} R_f(\overline{\theta}, r_1)\, dr_1, \tag{17}$$

where

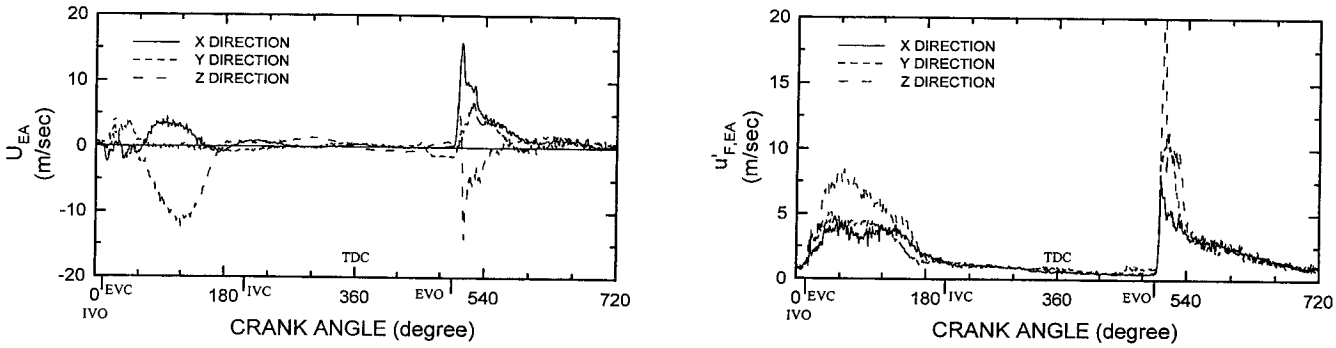

Fig. 5. The three components of (a) the mean velocity and (b) the fluctuation intensity at the central point.

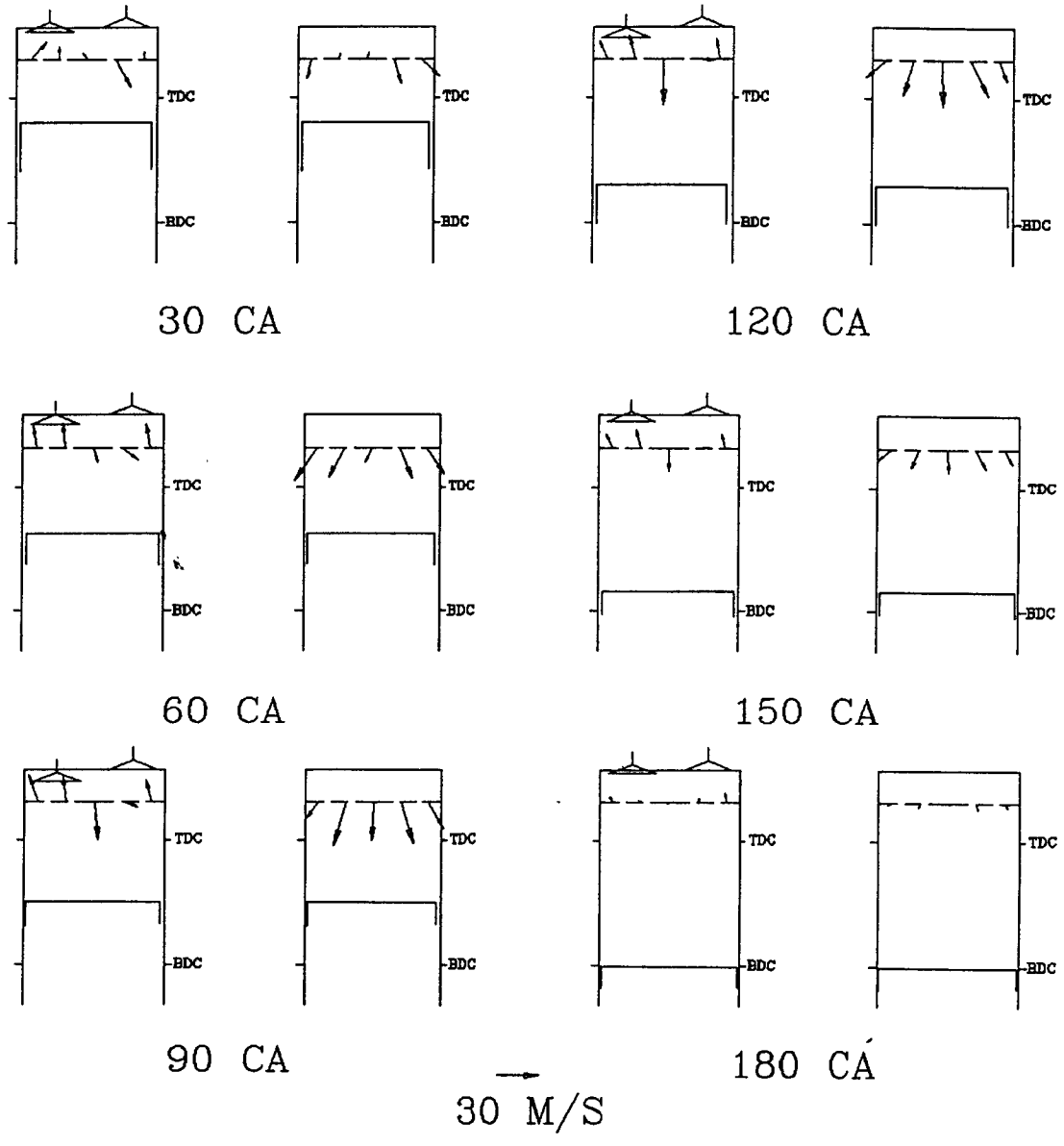

Fig. 6. The spatial distribution of the mean velocity on the *XZ* and *YZ* planes during the inlet stroke.

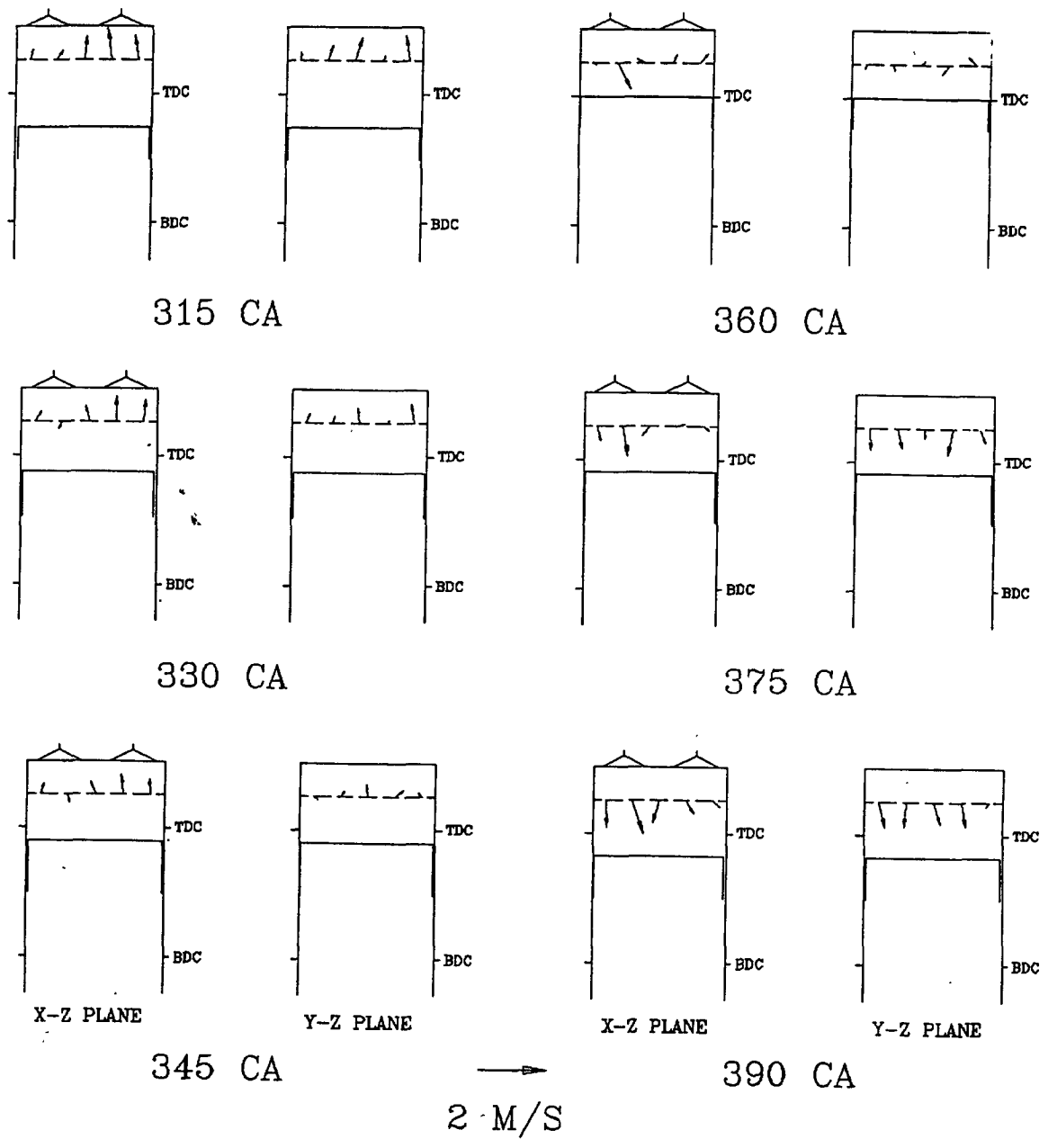

Fig. 7. The spatial distribution of the mean velocity on the *XZ* and *YZ* planes near the TDC during the closed period.

r_1^*: the first distance between the changeable point and the fixed point that makes $R_f(\overline{\theta}, r_1)=0$;

r_2^*: the first distance between the changeable point and the fixed point that makes $R_g(\overline{\theta}, r_2)=0$.

The above mathematical expressions indicate that the fluctuation velocity is no longer correlated when $r_1>r_1^*$ or $r_2>r_2^*$. The integral length scale evaluated using this technique is called the "direct length scale" in this paper.

IV. Results and Discussion

1. Single-Point Measurement

Using the traditional single point measurement, the three components of the mean and fluctuation velocity can be plotted as shown in Fig. 5. Note that the fluctuation velocity is always on the same magnitude order as, or even large than, the mean velocity.

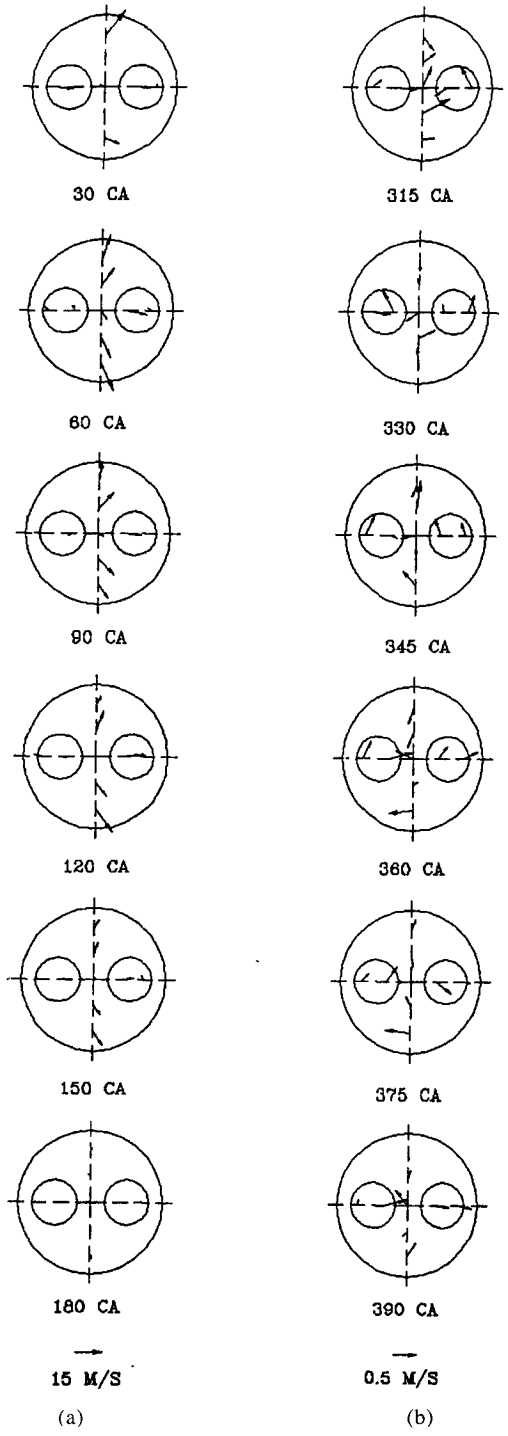

Fig. 8. The spatial distribution of the mean velocity on the *XY* plane during (a) the inlet stroke and (b) near the TDC during the closed period.

This implies that the flow is turbulence dominated. The three components of the mean velocity have their own characteristics. The *Z*-component is mainly influenced by the piston movement whereas the *X* and *Y* components depend upon the valve motion. The diagram shows that the flow is three-dimensional. The mean velocity varies with respect to the crank angle, which indicates that the turbulent flow is nonstationary.

Figure 6 shows the spatial relation of the direction and magnitude of the mean velocity on the *XZ* and *YZ* planes during the inlet stroke. Basically, the flow is induced from the inlet valve towards the piston head with an apparent recirculation zone which occurs beneath the inlet valve. The flow pattern is almost symmetric in the *YZ* plane. The mean flow velocity reaches its maximum in the middle of the inlet stroke (around 90 CA) and reduces to its minimum at the bottom dead center. During the compression stroke in the closed period, the flow velocity decreases to a much lower rate. (Note that the scaling has been changed in Fig. 7.) The moving piston starts to affect the flowfield. When it is close to the TDC, the flowfield appears to be three-dimensional without a fixed pattern except that the flow direction is the same as the piston moving direction. From the top view on the *XY* plane, the same results are displayed again in Fig. 8. It appears that the flow pattern is insymmetric with respect to the *X* and *Y* axes when the piston is close to the TDC. This is due to the fact that the inlet profile is very difficult to keep exactly symmetric in a real situation. A small disturbance in the inlet jet may cause the flow to change in pattern in the following compression stroke.

To evaluate the integral time and length scales from the single point measurement, the temporal autocorrelation coefficient has to be obtained first. Using the temporal autocorrelation coefficients versus the phase angle diagram, as shown in Fig. 9, the area below the fluctuation curves can be integrated following the definition of Eq. (12). However, the figure clearly shows that the fluctuation velocity has a reasonable rate of decay while the turbulence velocity decays rapidly. This implies that the magnitude of the integral time scale calculated from the cycle resolved method will be very small. That leads to a strange result when the integral length scale is calculated as shown in Fig. 10. Although the ensemble average time scale is more or less correct, the length scale transferred from the Taylor's hypothesis is very similar to the mean velocity diagram. This is not correct from a physical point of view. Direct measurement of the length scale is therefore necessary.

2. Two-Point Measurement

In order to measure the integral length scale

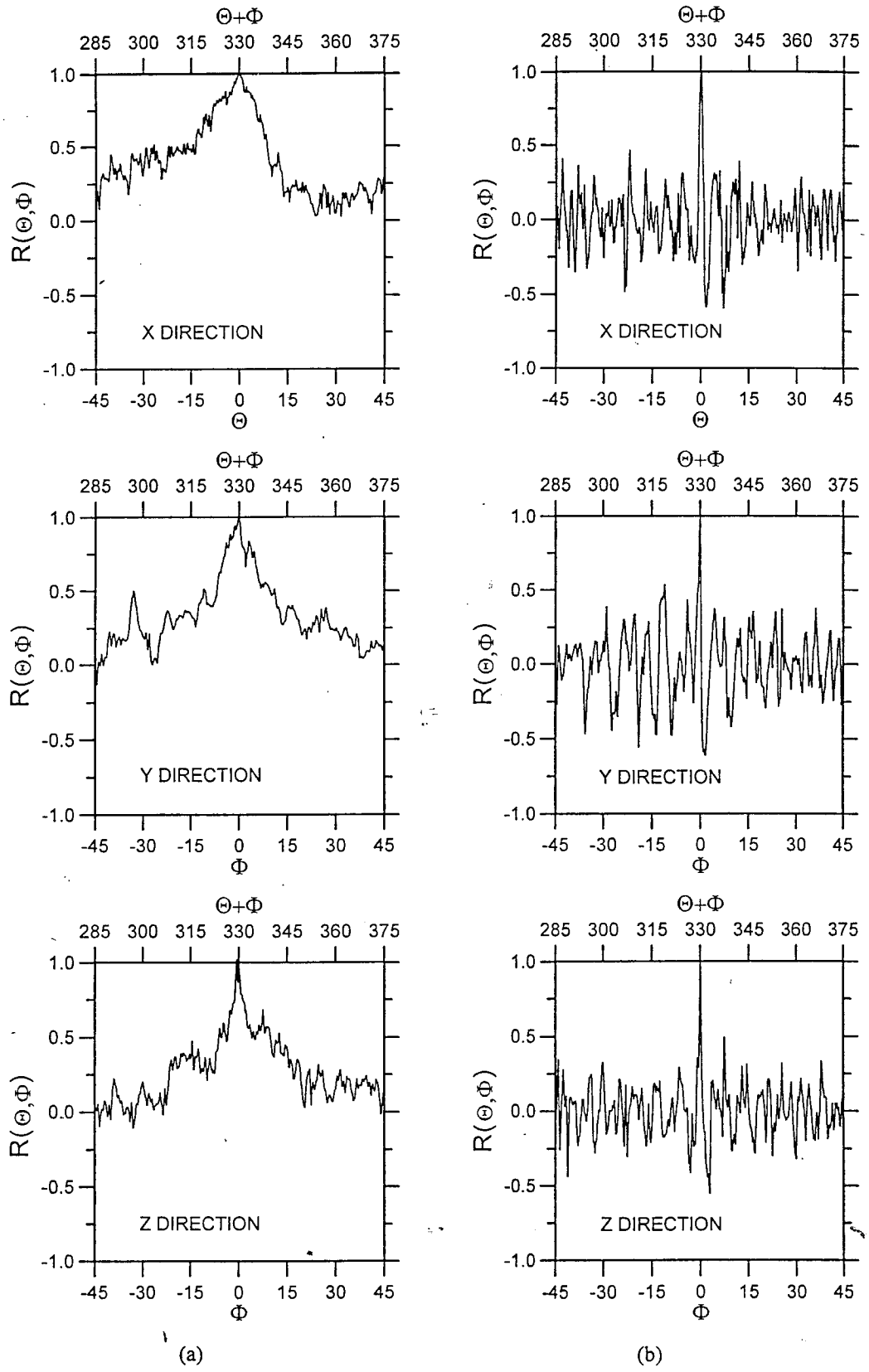

Fig. 9. Temporal autocorrelation coefficients versus the phase angle diagrams, using (a) the ensemble averaged fluctuation velocity and (b) the cycle-resolved turbulence velocity.

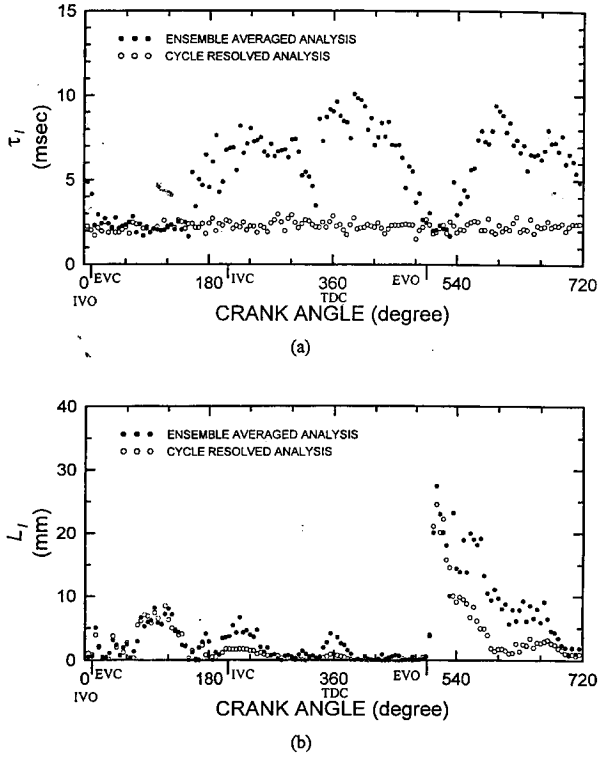

Fig. 10. Ensemble averaged analysis and cycle-resolved analysis used to evaluate (a) the integral time scale and (b) the integral length scale of the turbulence.

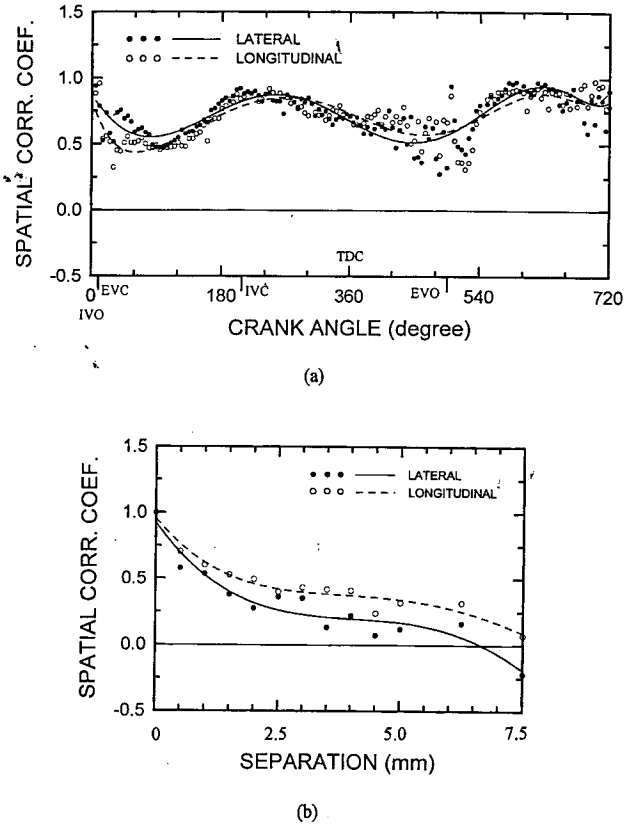

Fig. 11. (a) Spatial correlation coefficients versus the crank angle at a separation distance of 1 mm. (b) Spatial correlation coefficients versus the separation distance at a crank position of 360 CA.

directly, a two-point simultaneous measurement technique has to be used. The measurement was carried out at the central point for each separation distance (0.5 to 10 mm) and each crank angle. For example, at a separation distance of 1 mm, the spatial autocorrelation coefficients were measured and the results are shown in Fig. 11(a). The variation of the lateral and longitudinal coefficients versus the crank angle is related to the clearance height with a phase shift. A fourth order polynomial can be fitted to display the trend of the variation. The same data can be plotted again with respect to the separation distances. An example of a diagram of the spatial coefficients versus the separation distances at a crank position of 360 CA is displayed in Fig. 11(b). An exponential curve can be fitted to the variation. The area below the curve can be integrated to determine the length scale according to Eqs. (16) and (17).

Figure 12(a) shows a comparison of the length scales evaluated using the direct method (two-point measurement) and the indirect method (single-point measurement). If the direct length scale is regarded as the correct result, then the indirect length scale displays an incorrect trend of variation. However, the magnitude of the indirect length scale at the TDC is on the same order as the direct length scale (about 5 mm). Hence, the indirect method can be used to evaluate the length scale at the TDC for rough estimation. Figure 12(b) shows the lateral and longitudinal direct length scales with respect to the crank angle in the whole cycle. The longitudinal length scale is almost but not quite twice the lateral length scale near the TDC. This indicates that the in-cylinder turbulent flow field is neither isotropic nor homogeneous as assumed in the indirect method.

V. Conclusion

The in-cylinder turbulent flowfield of a reciprocating engine in the real situation is extremely complex. The investigation is far beyond a fundamental study. However, from experimental observation of the temporal and spatial characteristics, the following conclusions can be drawn.

(1)The in-cylinder flowfield is turbulent, nonstationary, and three dimensional. There

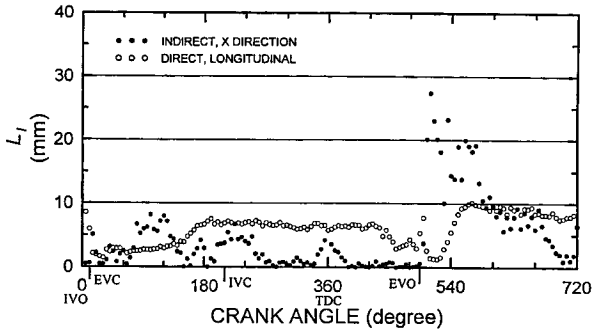

(a)

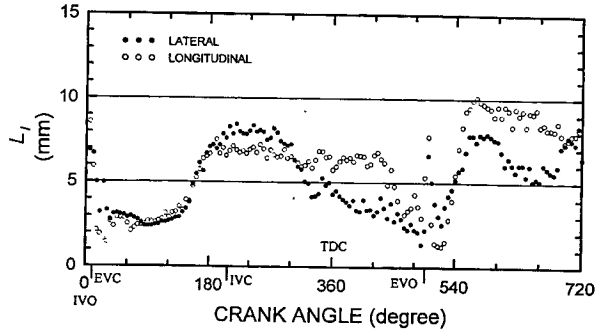

(b)

Fig. 12. (a) Comparison between the indirect and direct length scales. (b) Comparison between the direct lateral and longitudinal length scales.

exists an apparent recirculation zone beneath the inlet valve during the inlet stroke. The source of the in-cylinder turbulence is mainly the inlet turbulent jet for this pancake-type combustion chamber. The magnitude of the mean flow decreases to a much smaller value when the inlet valve is closed. The flow direction is mainly influenced by the piston movement during the compression and expansion strokes.

(2) Due to the restrictive assumptions of the Taylor's hypothesis (homogeneity, isotropy, and stationarity), the single-point measurement can be used only to obtain the integral time scale of the turbulence. To evaluate the integral length scale, the measurement technique has to employ the direct method.

(3) A two-point simultaneous measurement technique using a two-probe FLDV system has been devised in this study to measure the integral length scale directly. Statistical algorithms have been derived to analyze the fluctuating experimental results. Following a detailed experimental study at the central point, the results reveal a completely different trend compared with that estimated using the indirect method. This direct length scale is regarded as the correct answer. The experimental results can be used to validate in-cylinder computational results for model development.

Acknowledgment

Support from the NSC, R.O.C., under contract no. NSC 84-2212-E007-001 is gratefully acknowledged.

References

Abraham, J., R. D. Reitz, and F. V. Bracco (1985) Comparisons of computed and measured premixed charge engine combustion. *Combustion and Flame*, **60**, 309-322.

Cantania, A. E., C. Dongiovanni, and A. Mittica (1992) Time-frequency spectral structure of turbulence in an automotive engine. SAE Paper 920153, SAE International, Warrendale, PA, U.S.A.

Coz, J. F. L., S. Henriot, and P. Pinchon (1990) An experimental and computational analysis of the flow field in a four-valve spark ignition engine- focus on cycle-resolved turbulence. SAE Paper 900056, SAE International, Warrendale, PA, U.S.A.

Dinsdale, S., A. Roughton, and A. Mittica (1988) Length scale and turbulence intensity measurements in a motored I.C. engine. SAE Paper 880380, SAE International, Warrendale, PA, U.S.A.

Dyer, T. M. (1985) New experimental techniques for in-cylinder engine studies. SAE Paper 850396, SAE International, Warrendale, PA, U.S.A.

Fraser, R. A. and F. V. Bracco (1988) Cycle-resolved LDV integral length scale measurements in an I.C. engine. SAE Paper 880381, SAE International, Warrendale, PA, U.S.A.

Fraser, R. A. and F. V. Bracco (1989) Cycle-resolved LDV integral length scale measurements investigating clearance height scaling, isotropy and homogeneity in an I.C. engine. SAE Paper 890615, SAE International, Warrendale, PA, U.S.A.

Glover, A. R., G. E. Hundleby, and O. Hadded (1988a) The development of scanning LDA for the measurement of turbulence in engines. SAE Paper 880378, SAE International, Warrendale, PA, U.S.A.

Glover, A. R., G. E. Hundleby, and O. Hadded (1988b) An investigation into turbulence in engines using scanning LDA. SAE Paper 880379, SAE International, Warrendale, PA, U.S.A.

Han, Z , R. D. Reitz, F. E. Corcione, and G. Valentino (1996) Interpretation of k-ε computed turbulence length scale predictions for engine flows. 26th Symposium on Combustion, Combustion Institute, Pittsburgh, PA, U.S.A.

Heywood, J. B. (1987) Fluid motion within the cylinder of internal combustion engines — the 1986 Freeman scholar lecture. *ASME Transaction Journal of Fluids Engineering*, **109**, 3-35.

Hinze, J. O. (1975) *Turbulence*, 2nd Ed. McGraw-Hill, New York, NY, U.S.A.

Hong, C. W. and G. Y. Huang (1995) In-cylinder turbulent flow field measurement of a single cylinder transparent engine using FLDV. *J. of the Chinese Soc. of Mech. Engr.*, **16**(5), 457-466.

Hong, C. W. and C. H. Tzeng (1996) Parametric studies of in-cylinder pre-combustion turbulent flow field of a transparent engine using FLDV. *J. of the Chinese Inst. of Engr.*, **19**(1), 887-897.

Ikegami, M., M. Shioji, D. Y. Wei, and M. Sugiura (1985) In-cylinder measurements of turbulence by laser homodyne principle. *COMODIA 85 Symposium*, pp. 115-123. Tokyo, Japan.

Ikegami, M., M. Shioji, and K. Nishimoto (1987) Turbulence in-

tensity and spatial integral scale during compression and expansion strokes in a four-cycle reciprocating engine. SAE Paper 870372, SAE International, Warrendale, PA, U.S.A.

Kong, S. C. and C. W. Hong (1997) Multidimensional intake flow modeling of a four-stroke engine with comparisons to flow velocity measurements. SAE Paper 970883, SAE International, Warrendale, PA, U.S.A.

Liou, T. M. and D. A. Santavicca (1983) Cycle resolved turbulence measurements in a ported engine with and without swirl. SAE Paper 830419, SAE International, Warrendale, PA, U.S.A.

Liou, T. M., M. J. Hall, D. A. Santavicca, and F. V. Bracco (1984) Laser Doppler velocimetry measurements in valved and ported engines. SAE Paper 840375, SAE International, Warrendale, PA, U.S.A.

Liou, T. M. and D. A. Santavicca (1985) Cycle resolved LDV measurements in a motored I.C. engine. *ASME Transaction Journal of Fluids Engineering*, **107**, 232-240.

Reynolds, W. C. (1980) Modeling of fluid motions in engines – an introduction overview. In: *Combustion Modeling in Reciprocating Engines*, J.N. Mattavi and C.A. Amann Eds. Plenum Press, New York, NY, U.S.A.

Sweetland, P. and R. D. Reitz (1994) Particle image velocimetry measurements in the piston bowl of a DI diesel engine. SAE Paper 940283, SAE International, Warrendale, PA, U.S.A.

Tennekes, H. and J. L. Lumley (1972) *A First Course in Turbulence*. The MIT Press, Cambridge, MA, U.S.A.

Witze, P. O. (1980) A critical comparison of hot wire anemometry and laser Doppler velocimetry for I.C. engine applications. SAE Paper 800132, SAE International, Warrendale, PA, U.S.A.

透明引擎缸內紊流流場時間空間特性雷射量測分析

洪哲文　陳德記

國立清華大學動力機械學系

摘　要

本篇論文描述由清華大學內燃引擎燃燒實驗室所發展之量測引擎缸內非穩態紊流流場時空特性之軟硬体技術。硬体上，引擎氣缸被改成透明，而一台原二光纖探管之三維雷射測速儀被設計改裝成一兩點同時量測之紊流積分長度尺度量測設備。單點三維量測及雙點單維量測可同時進行。軟体上，循環變異之統計技巧被應用於分析此非穩態紊流流場，其時空特性與物理意義解釋爲本論文重點